Supporting Information

Visible Light-Driven H$_2$ Production over Highly Dispersed Ruthenia on Rutile TiO$_2$ Nanorods

Thuy-Duong Nguyen-Phan,[1] Si Luo,[1,2] Dimitriy Vovchok,[1,2] Jordi Llorca,[3] Jesús Graciani,[4] Javier Fernández Sanz,[4] Shawn Sallis,[5] Wenqian Xu,[6] Jianming Bai,[7] Louis F. J. Piper,[5] Dmitry E. Polyansky,[1] Etsuko Fujita,[1] Sanjaya D. Senanayake,[1] Dario J. Stacchiola,[1]* and José A. Rodriguez[1,2]*

[1] Chemistry Department, and [7] Photon Sciences Division, Brookhaven National Laboratory, Upton, NY 11973, US

[2] Department of Chemistry, Stony Brook University, Stony Brook, NY 11790, US

[3] Institute of Energy Technologies and Centre for Research in NanoEngineering, Universitat Politècnia de Catalunya, Diagonal 647, 08028 Barcelona, Spain

[4] Department of Physical Chemistry, University of Seville, E-41012, Seville, Spain

[5] Materials Science & Engineering, Department of Physics, Applied Physics and Astronomy, Binghamton University, Binghamton, NY 13902, US

[6] Advanced Photon Source, Argonne National Laboratory, Argonne, Illinois 60439, US

CHARACTERIZATIONS

The scanning electron microscopy (SEM) images were taken on a Hitachi S-4800 microscope. The energy-dispersive X-ray spectroscopy (EDS) spectrum and elemental mapping were acquired on a JEOL 7600F high resolution analytical SEM. The photoluminescence (PL) spectroscopy was recorded by an ISS^{TM} PC1/K2 Photon Counting Spectrofluorometer with ISS-PC1 as excitation light source (set the excitation wavelength at 325 nm) and a photomultiplier tube (Hamamatsu R928) as a detector. All these facilities are supported by the Center for Functional Nanomaterials (CFN) at BNL.

VISIBLE-LIGHT-DRIVEN H$_2$ PRODUCTION MEASUREMENTS

The photocatalytic water splitting activity was evaluated through the measurement of hydrogen evolution in a closed gas circulation and evacuation system. 3 mg of powder catalyst were suspended in 3 mL of aqueous methanol solution (20 vol%) in a 6-mL sealed quartz cell. After evacuation and Ar purging several times to remove the dissolved oxygen in the solution ensuring the anaerobic condition, the reactor was side-irradiated by a 150 W Xenon arc lamp from Optical Building Blocks Corporation equipped with a CuSO$_4$ filter and 400 nm long pass filter (Thorlabs, Inc.) (400 nm $< \lambda <$ 625 nm) under magnetic stirring. The light intensity was 475 mW over an irradiated area of 1.13 cm^2 (determined by an optical power meter from Ophir Optronics). The reaction temperature was maintained at 293 K by continuous water circulation. The evolved gases were determined by gas chromatography (GC Agilent 6890N) equipped with FID and TCD detectors using Ar as the carrier gas.

CALCULATION OF APPARENT QUANTUM EFFICIENCY (AQE)

As shown in Table S1, the wavelength range of 150 W Xe arc lamp equipped with aqueous $CuSO_4$ filter is from 310 to 625 nm. The light intensity over the entire range is 750 mW cm^{-2} and the irradiated area (S) of 1.13 cm^2. The energy in each photon is given by:

$$E = \frac{hc}{\lambda} \text{ [joules]}$$

where h is Planck's constant (6.626 * 10-34 J s)

    c is speed of light (2.998 * 108 m s^{-1})

    λ is wavelength [nm]

So the number of photons per joule is:

$$N_{p\lambda} = \lambda * 5.03 * 10^{15}$$

Total photons per second were determined by the following equation:

$$N_{p\lambda} = \alpha \int_{310}^{625} S * I_{\lambda} * 5.03 * 10^{15} * d\lambda$$

where S is the irradiated area [m^2]

    I_{λ} is the spectral irradiance [W m^{-2} nm^{-1}]

    α is conversion factor

Total moles of photons (einsteins) per second (2.85 E-06) was obtained by dividing total photons per second by Avogadro constant (NA = $6.022*10^{23}$).

Two electrons are required to produce one H_2 molecule; therefore the apparent quantum efficiency was calculated using the following equation:

$$AQE\% = \frac{\text{number of reacted electrons}}{\text{number of incident photons}} * 100 = \frac{\text{number of evolved } H_2 \text{ molecules} * 2}{\text{number of incident photons}} * 100$$

For example, the rate of H_2 production over 0.1RuTi sample was determined to be 9.9 μmol h^{-1} under UV-Vis irradiation, thus the AQE for H_2 production in range of 310-625 nm was calculated as follows:

$$AQE\% = \frac{\dfrac{2*9.9*10^{-6}}{60*60}}{2.85*10^{-6}}*100 = 0.194\%$$

Table S1. Parameters for quantum efficiency calculation.

Wavelength range / nm	Irradiated area / m^2	Total power / mW	Total photons per sec	Total einsteins per sec
310 ~ 625 nm	1.13E-4	750	1.71E+18	2.85E-06
400 ~ 625 nm	1.13E-4	475	1.15E+18	1.91E-06

Supporting figures

Figure S1. (A) Time profiles of H_2 production and (B) gas evolved rate over TiO_2 and xRuTi series under UV-visible irradiation ($\lambda = 310 \sim 625$ nm).

Figure S2. (A, B) Time curves and (C) rates of H_2 evolution over 0.1RuTi, 0.1PtTi and ternary 0.1Pt0.1RuTi under the irradiation of UV-visible and visible light, respectively.
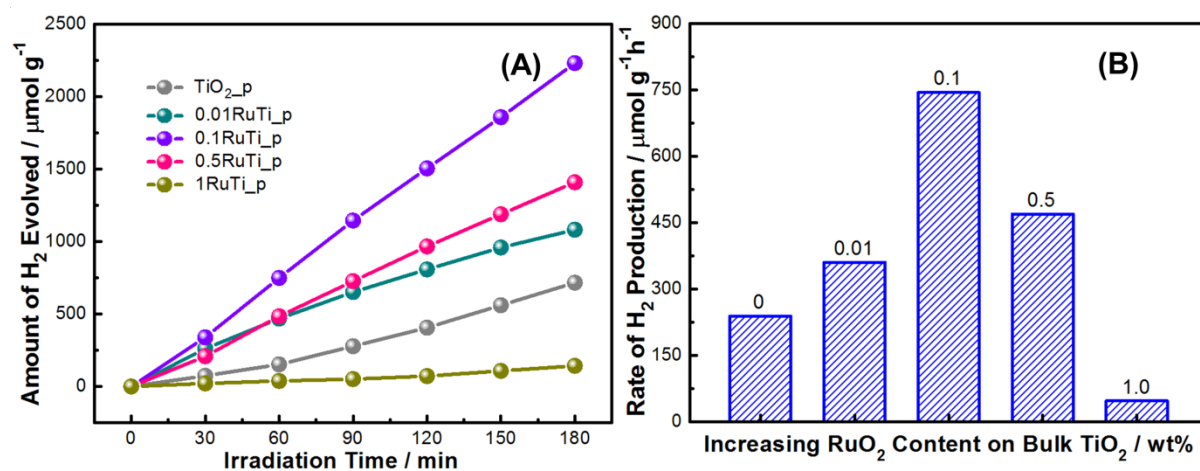
Figure S3. H_2 production performance under UV-visible irradiation (310 nm ~ 625 nm) of TiO$_2$_p and RuO$_2$ loaded on TiO$_2$_p with different RuO$_2$ contents.

Figure S4. Rietveld refinement of TiO$_2$ and xRuTi series.

Figure S5. (A) Crystal structure of rutile TiO_2, anatase TiO_2 and λ-Ti_3O_5 (blue and red balls are Ti and O, respectively); (B) XRD patterns; and (C) photoactivity comparison between TiO_2, treated TiO_2 (containing TiO_2 and λ-Ti_3O_5) and 0.1RuTi heterostructure (methanol as sacrificial agent, 150 W Xe arc lamp, 310 nm $< \lambda <$ 625 nm). It is obvious that the performance of TiO_2 and treated TiO_2 was likely identical, demonstrating no contribution of λ-Ti_3O_5 to the photocatalytic H_2 evolution.

Figure S6. (A, B) SEM, (C) HR-TEM and (D) HAADF-STEM images of pure TiO_2 rods.
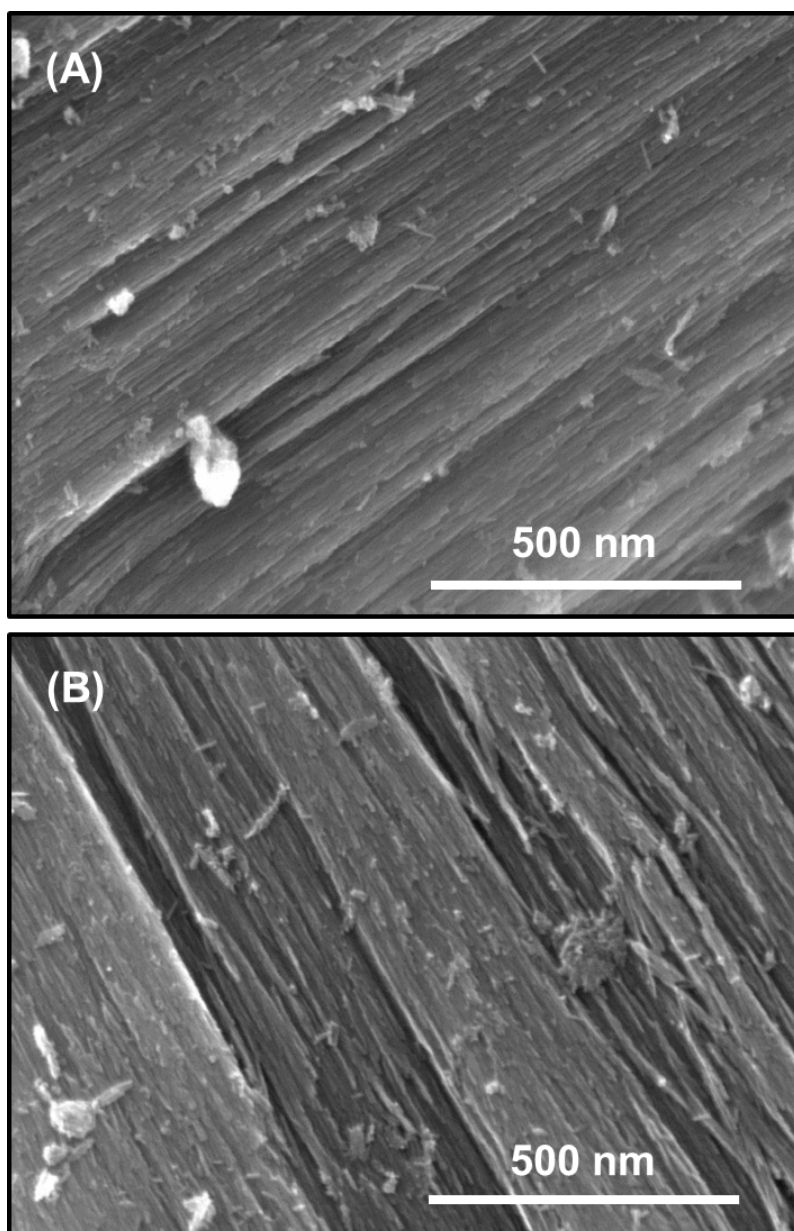
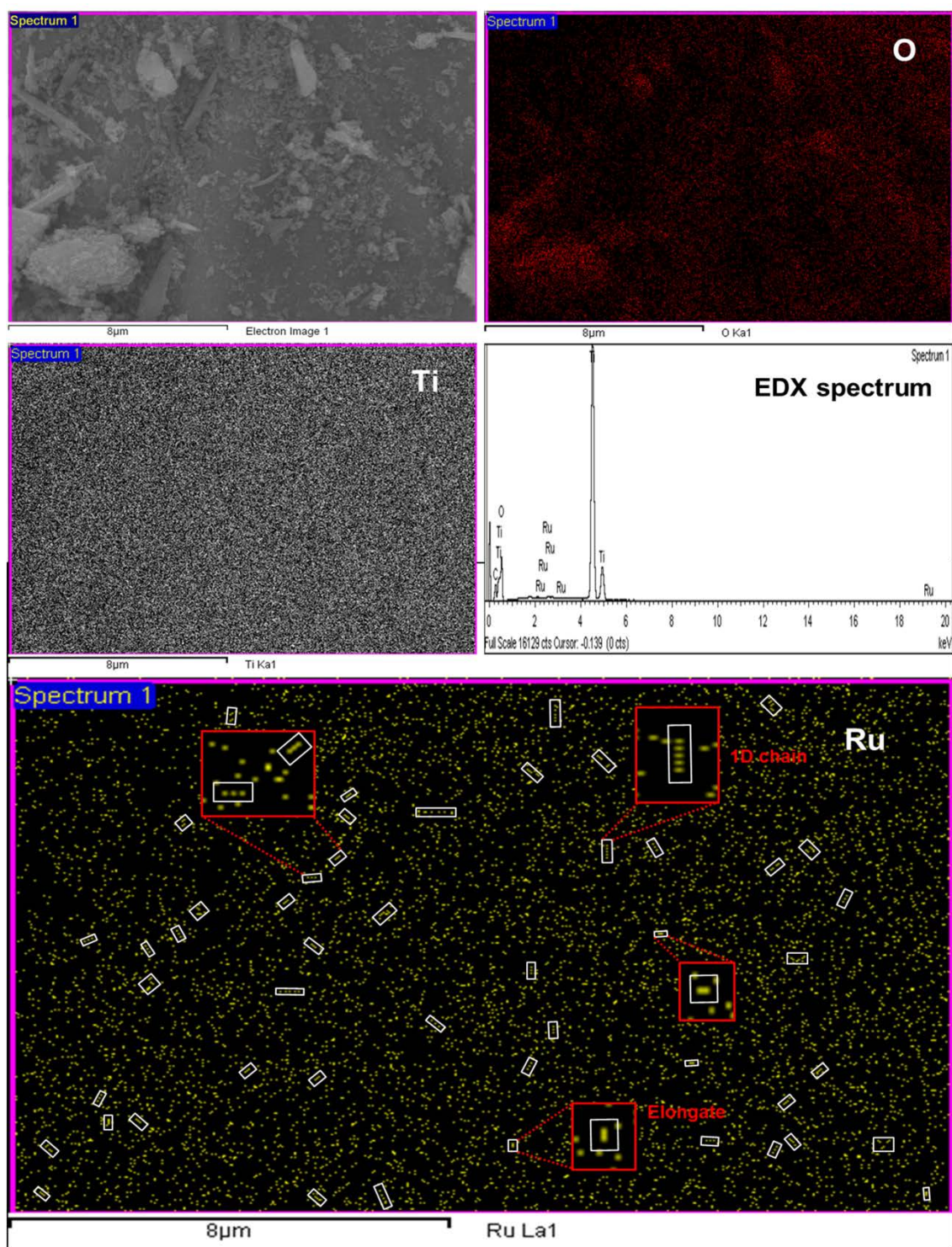**Figure S7.** SEM images of (A) 0.01RuTi and (B) 0.5RuTi materials.

Figure S8. SEM/elemental mapping of 0.1RuTi sample. Carbon in EDX spectrum originates from carbon tape for powder mounting. White rectangles in Ru map show different geometries of Ru signals and red rectangles indicate magnified images of elongated and 1D chain-like features apart from spherical-like geometry.
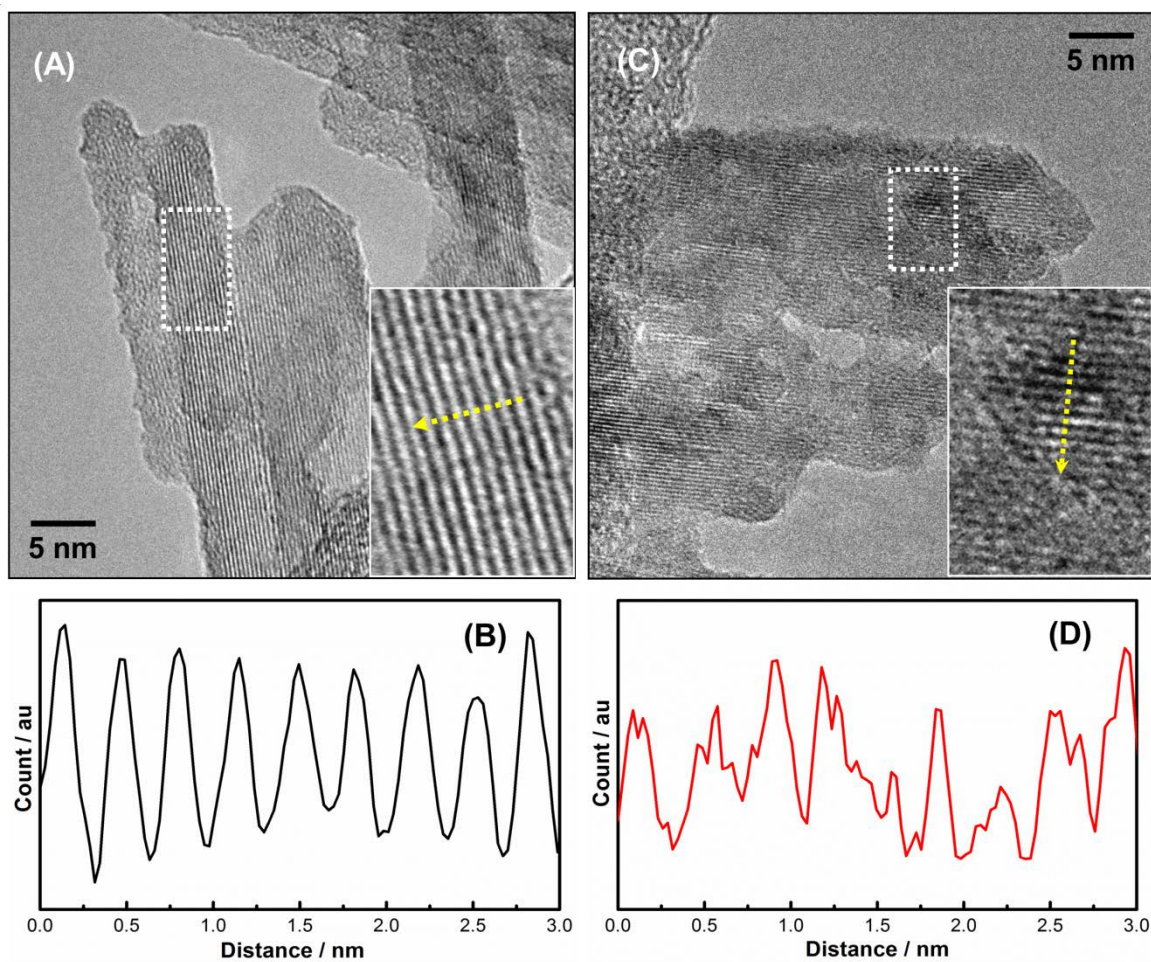
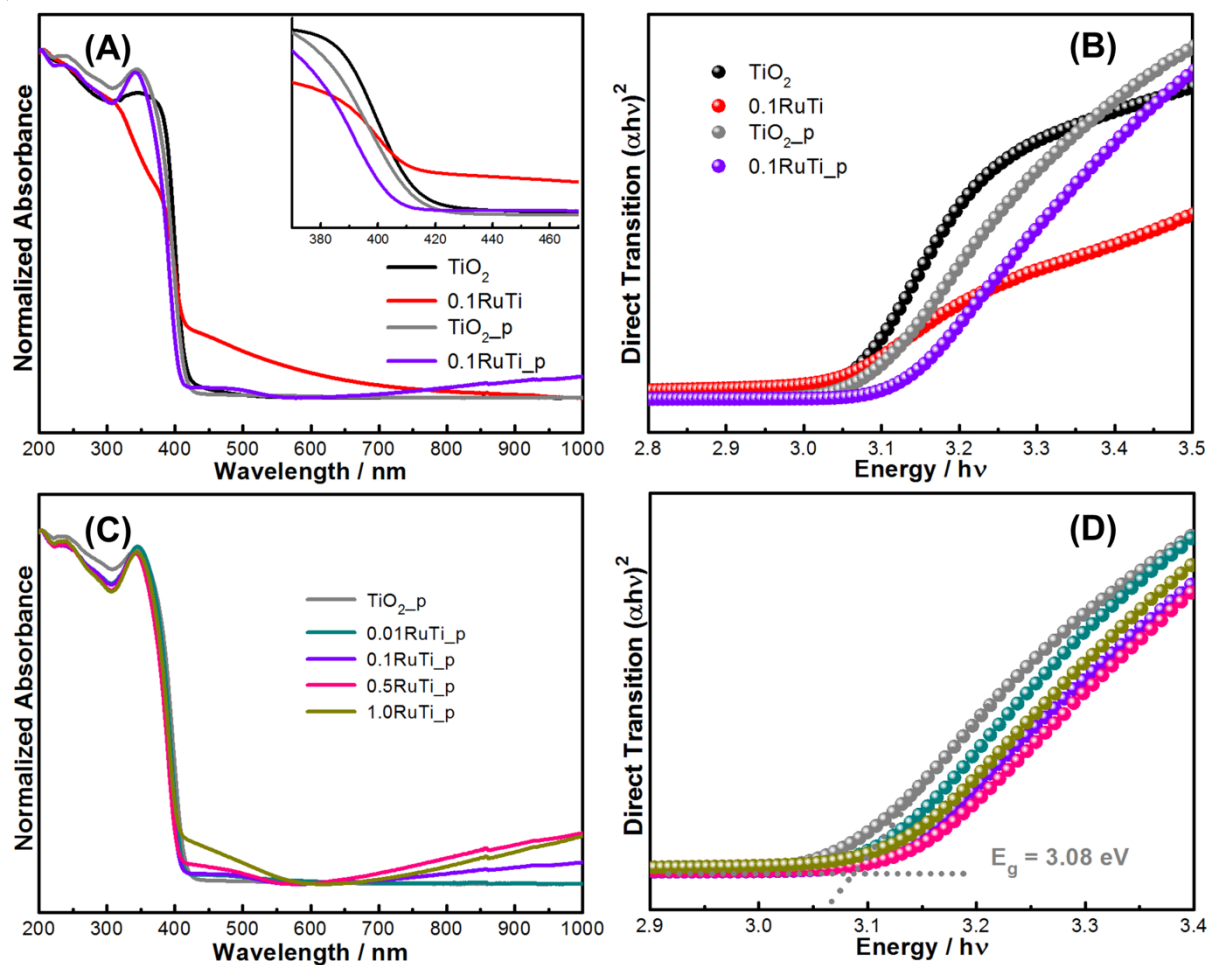**Figure S9.** Lattice fringe analysis from HR-TEM images of (A, B) TiO$_2$ NRs and (C, D) 0.1RuTi.

Figure S10. (A, C) UV-Vis-DRS spectra and (B, D) corresponding Tauc's plots of TiO_2_p and RuTi_p series with different RuO_2 contents.
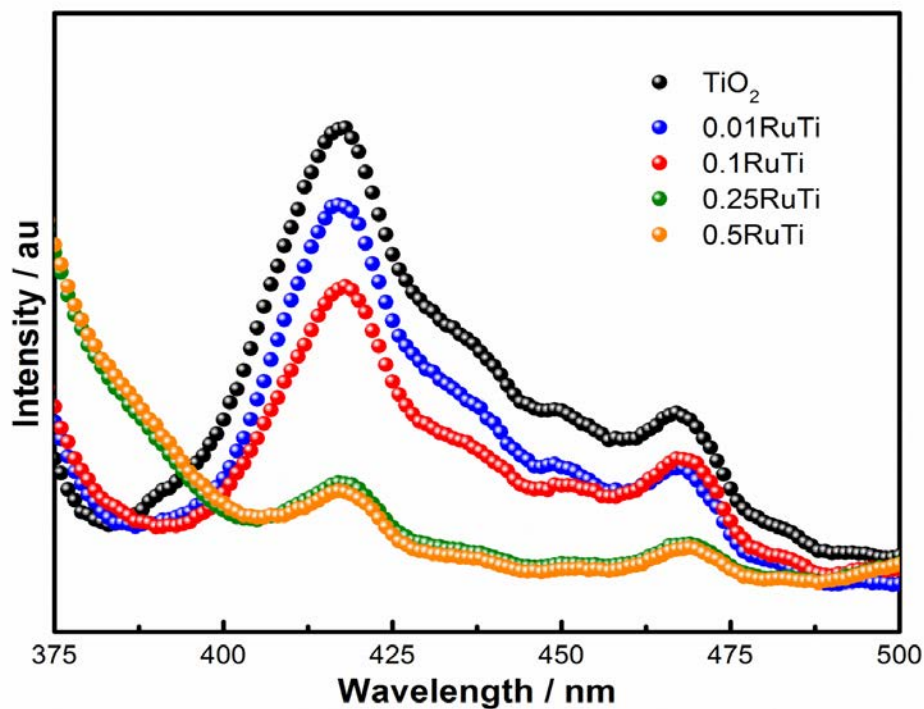
Figure S11. PL spectra of TiO₂ NRs and xRuTi systems (excitation at 325 nm). The major emission peaks at 418 nm (2.97 eV) can be ascribed to the emission of band gap transition of rutile. Much smaller peak at 467 nm (2.65 eV) and two shoulders at 436 nm (2.84 eV) and 450 nm (2.76 eV) correspond to the free excitons at the band edge.
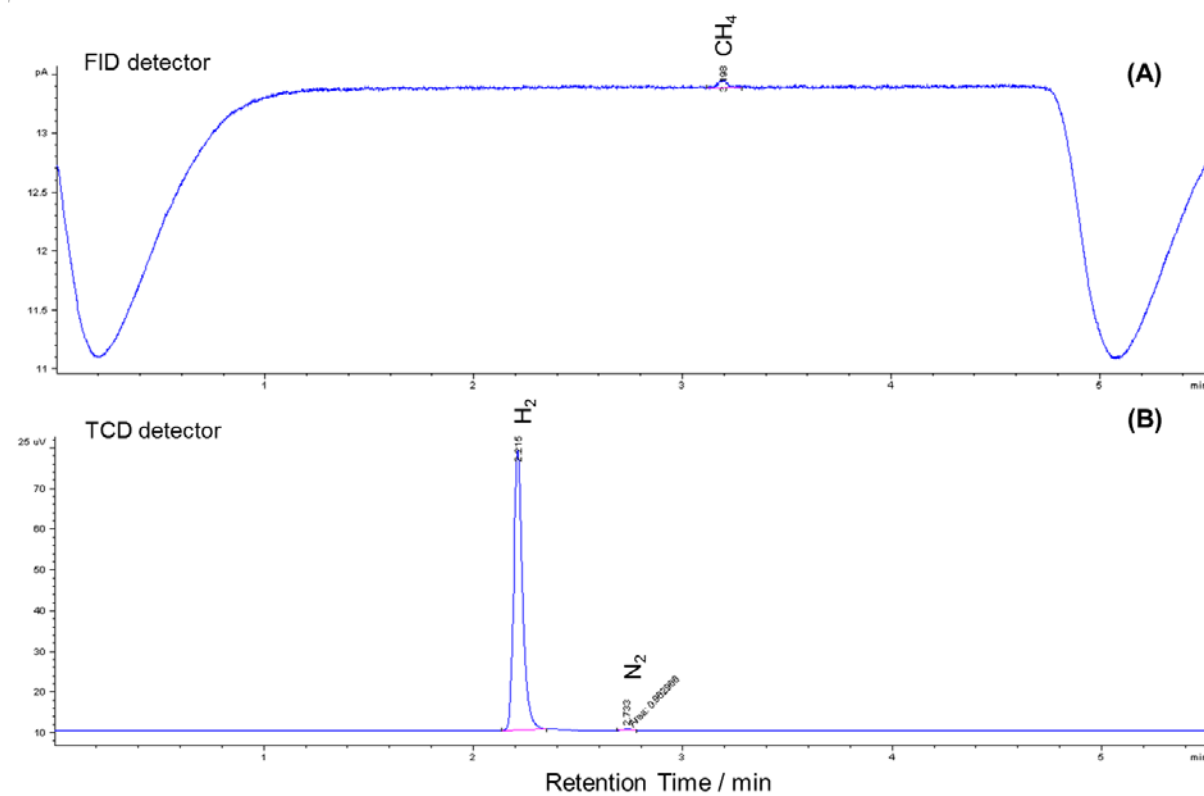
Figure S12. Gas chromatography spectra for gas product analysis: (A) FID signal and (B) TCD signal.